Electron Momentum Distribution in Titanium and the Renormalized-Free-Atom Model

K.-F. Berggren
Department of Physics, University of Linköping, S-581 83 Linköping, Sweden

S. Manninen and T. Paakkari
Department of Physics, University of Helsinki, Siltavuorenpenger 20C, SF-00170 Helsinki, Finland
(Received 1 March 1973)

The Compton profile of polycrystalline titanium has been measured using 59.54-keV γ rays from a ^{241}Am source. The resulting Compton profile is significantly different from Weiss's previous measurements obtained form Mo$K\alpha$ and Ag$K\alpha$ radiation. Our experimental results have been interpreted by means of a renormalized-free-atom model. Good agreement between measured and computed quantities is found if the electronic configuration is chosen as $3d^3\,4s^1$ (in atomic notations), which is to be compared with the atomic configuration $3d^2\,4s^2$.

Recently one of us[1] used a renormalized-free-atom (RFA)[2-4] model and calculated the electron momentum distribution in vanadium. A good agreement with the experimental data[5] at low momenta with the electronic configuration $3d^4\,4s^1$ (in atomic notations) prompted us to study other transition metals. In this paper we report an experimental Compton profile of polycrystalline titanium and interpret it by means of an RFA model. The case of titanium has also been investigated by Weiss.[6] We find, however, our observed and computed values to be in substantial agreement, which suggests the essential accuracy of our $3d^3\,4s^1$ electronic configuration.

The experimental technique reported previously[5] was revised in a few aspects. A strong 900-mCi ^{241}Am source with a diameter of 12 mm was used to obtain 59.54-keV photons. Because of the large size of the source, the incident beam was collimated to $\pm 1°$ by a Soller slit made of Mo sheets. The scattering angle from a compact of titanium powder in a vacuum chamber was 150°. The divergence of the scattered beam in the plane of scattering was further limited to $\pm 2°$ by another Soller slit.

The peak-to-background ratio in the experiment was 200 to 1 and we ascertained that the background consisted solely of γ rays and cosmic radiation which came through the lead shield. The stability of the detecting system (amplifier, 716A Ortec; analog-to-digital converter, ND/560; multichannel analyzer, ND 2400) was found to be better than 0.2 channels at 59.54 keV during the measuring period of 2 days. During that time about 6000 counts were accumulated into a channel at the Compton peak with a 63.2-eV separation between the channels of the multichannel analyzer.

After the subtraction of the background, the results were corrected for instrumental resolution [540-eV full width at half-maximum (FWHM) at 59.54 keV] and for the absorption of γ rays in the sample. The effect of the relativistic correction was taken into account by dividing the measured intensity $I(E_2)$ by the correction for the energy dependence of the relativistic Compton cross section.[7] Finally, the results were converted from the energy scale of the scattered photon, E_2 (eV), to an electron momentum scale, p_z (a.u.). The $p_z = 0$ point was determined by fitting a parabola at the peak of the Compton line, and the areas under the halves of the profile were each normalized to correspond to the contribution of 11 electrons, i.e., one-half of the total number of electrons per titanium atom. The final results for the normalized and centered Compton profile for Ti are given in Table I and in Figs. 1 and 2. These results are for the high-energy half of the Compton profile, though both sides of the profile agreed well throughout the region of

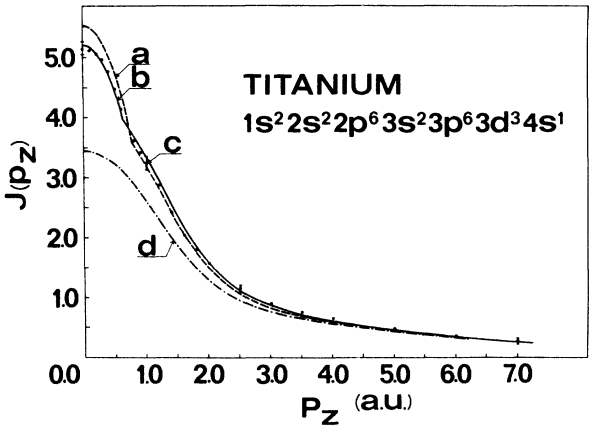

FIG. 1. Experimental and calculated Compton profiles of polycrystalline titanium: (a) calculated from the RFA model with a configuration $1s^2 \cdots 3d^2\,4s^2$, (b) calculated from the RFA model with a configuration $1s^2 \cdots 3d^3\,4s^1$, (c) experimental results (the statistical error is indicated for some points), and (d) contributions from the core states $1s^2 \cdots 3p^6$.

TABLE I. Compton profile of polycrystalline titanium.

p_z (a.u.)	$1s^2\cdots3p^6$	$3d^1$	$1s^2\cdots3d^3$ +free-electron gas	Weiss[a] expt.	present expt.	RFA $3d^3 4s^1$
0.0	3.449	0.270	5.45	5.43 ± 0.15	5.14 ± 0.10	5.22
0.1	3.441	0.270	5.41	···	5.12	5.19
0.2	3.416	0.270	5.30	5.32	5.07	5.10
0.3	3.376	0.270	5.10	···	4.97	4.95
0.4	3.317	0.270	4.83	5.11	4.78	4.72
0.5	3.240	0.267	4.48	···	4.48	4.43
0.6	3.145	0.262	4.04	4.68	4.15	4.07
0.7	3.033	0.255	3.80	···	3.88	3.86
0.8	2.907	0.246	3.65	3.84	3.63	3.70
0.9	2.770	0.235	3.48	···	3.43	3.53
1.0	2.625	0.222	3.29	3.14	3.26 ± 0.10	3.35
1.2	2.322	0.194	2.90	2.58	2.89	2.95
1.4	2.025	0.165	2.52	2.28	2.43	2.55
1.6	1.750	0.137	2.16	1.96	2.05	2.18
1.8	1.511	0.112	1.85	1.65	1.81	1.85
2.0	1.311	0.091	1.59	1.43 ± 0.10	1.58	1.59
2.5	0.967	0.054	1.13	···	1.17 ± 0.06	1.13
3.0	0.774	0.032	0.87	···	0.90	0.87
3.5	0.657	0.019	0.71	···	0.76	0.71
4.0	0.572	0.011	0.61	0.52	0.65	0.61
5.0	0.438	0.004	0.45	0.39	0.46	0.45
6.0	0.331	0.002	0.34	0.30	0.35	0.34
7.0	0.249	0.001	0.25	0.13 ± 0.02	0.27 ± 0.03	0.25

[a]R. J. Weiss, Ref. 6. ($1s^2$ of Ti not excited.)

$p_z = \pm 7.0$. The high-energy side of the profile can be considered more reliable because of the smaller effects of resolution and because of the lack of low-intensity lines due to the impurities of the Am source used.

To interpret the experimental data we will focus on the low-momentum region in which the crystalline effects are most pronounced. In principle, the Compton profile could be derived from a full band-structure calculation. As was shown in the case of vanadium,[1] however, we do not have to go that far in computational efforts in order to simulate the experimental situation. The elementary RFA[1-4] model, which makes an appealing compromise between a free-atom calculation and a rigorous band-structure description, seems to bring out the essential effects of the crystalline environment and enables us to make conclusions about the electronic configuration of the transition metals.

In the RFA model, approximate crystal wave functions are derived by truncating the free-atom Hartree-Fock wave functions at R_0 of the Wigner-Seitz sphere and renormalizing them to 1 within this sphere. In the usual cell approximation we then have for the 4s band, for example, the crystal wave functions

$$\phi_{\vec{k}}(\vec{r}) = e^{i\vec{k}\cdot\vec{r}}\phi_0(\vec{r}) , \quad (1)$$

where ϕ_0 is the renormalized free-4s-atom wave function. Assuming a spherical occupation up to p_F, the momentum density per atom associated with the 4s band may then be written for a hcp crystal as

$$\rho(\vec{p}) = 2 \sum_{|\vec{p}-\vec{K}_n| \le p_F} |\phi_0^c(\vec{K}_n)|^2 [1 + \cos(\vec{K}_n \cdot \vec{\tau})]/2 , \quad (2)$$

where $\vec{\tau}$ determines the position of an atom in the

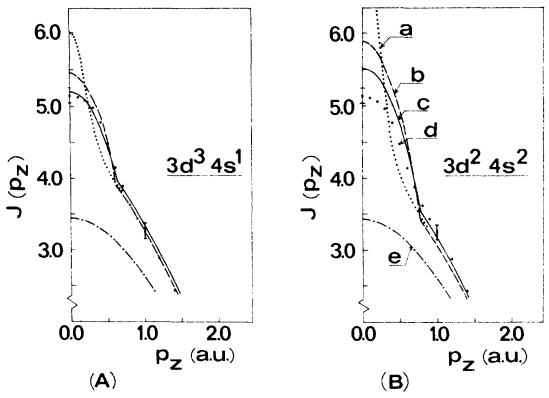

FIG. 2. Experimental and calculated Compton profiles at low momenta for the configurations (A) $3d^3 4s^1$ and (B) $3d^2 4s^2$: (a) calculated with an atomic 4s function plus core states, (b) calculated with a free-electron 4s band plus core states, (c) calculated from the RFA model, (d) experimental results, and (e) contributions from the core states $1s^2\cdots3p^6$.

unit cell, $\vec{K}_n$ is a reciprocal-lattice vector, and

$$\phi_0^c(\vec{K}_n) = (2\pi)^{-3/2} \int_{\Omega_0} d\vec{r}\, \phi_0(\vec{r})\, e^{-i\vec{K}_n\cdot\vec{r}}. \quad (3)$$

The integration in Eq. (3) is over an atomic cell, which with some caution may be replaced by a sphere.[1] It is straightforward to take a spherical average $\langle \rho(\vec{p}) \rangle$ of Eq. (2) and to derive the Compton profile, which in the impulse approximation reads

$$J(p_z) = 2\pi \int_{p_z}^{\infty} dp\, p \langle \rho(\vec{p}) \rangle . \quad (4)$$

For hcp structure we obtain

$$J_{4s}(p_z) = 4\pi \sum_{n=0}^{\infty} |\phi_0^c(K_n)|^2 G_n(p_z) . \quad (5)$$

For $n \neq 0$ we have

$$G_n(p) = \begin{cases} 0 , & p > K_n + p_F \\ \tilde{G}_n(p) , & p \in (K_n - p_F,\ K_n + p_F) \\ \tilde{G}_n(K_n - p_F) , & p < K_n - p_F \end{cases} \quad (6)$$

where

$$\tilde{G}_n(x) = \tfrac{1}{2} N_n \langle 1 + \cos(\vec{K}_n\cdot\vec{\tau}) \rangle \times \{(p_F^2 - K_n^2)(K_n + p_F - x) - \tfrac{1}{3}[(K_n + p_F)^3 - x^3] + K_n[(K_n + p_F)^2 - x^2]\}/4K_n . \quad (7)$$

N_n is the number of points in the nth shell in reciprocal space and $\langle \cdots \rangle$ denotes an average over this shell. For $n = 0$ in Eq. (5) we simply have

$$G_0(p) = \tfrac{1}{2}(p_F^2 - p^2) . \quad (8)$$

Because the 4s atomic function is by far the most extended one, the dominant crystalline effects are to be found in $J_{4s}(p_z)$ in Eq. (5); only 34% of Clementi's[8] 4s function for Ti is within the Wigner-Seitz sphere, which is to be compared with 96% for the 3d function. For this reason it should be acceptable to neglect the presumably minor renormalization effects on the d states and to treat these states as being atomic. In the calculations we have used Clementi's[8] atomic Hartree-Fock wave functions, and the results are given in Table I and in Figs. 1 and 2. Considering the limits of error in the experimental data, we regard the agreement between theory and experiment as satisfactory. The gross features of the experimental Compton profile are indeed described by our model. We feel that when experimental accuracy has been sufficiently improved then the consideration of smaller effects such as renormalization of d states, band-structure effects, and electron-electron correlation may well become important. In conclusion, it is evident from Fig. 2 that the electronic configuration in titanium metal is close to $3d^3\,4s^1$ (in atomic notations) rather than $3d^2\,4s^2$.

---

[1] K.-F. Berggren, Phys. Rev. B **6**, 2156 (1972).

[2] R. E. Watson, H. Ehrenreich, and L. Hodges, Phys. Rev. Lett. **24**, 829 (1970).

[3] R. E. Watson and H. Ehrenreich, Comments Solid State Phys. **3**, 109 (1970).

[4] L. Hodges, R. E. Watson, and H. Ehrenreich, Phys. Rev. B **5**, 3953 (1972).

[5] T. Paakkari, S. Manninen, O. Inkinen, and E. Liukkonen, Phys. Rev. B **6**, 351 (1972).

[6] R. J. Weiss, Phys. Rev. Lett. **24**, 883 (1970); Philos. Mag. **25**, 1511 (1972).

[7] The relativistic correction used in this paper differs slightly from the one calculated by P. Eisenberger and W. A. Reed, Phys. Rev. A **5**, 2085 (1972). In their notations we have used an approximation $d^2\sigma/d\omega_2\, d\Omega_2 = (r_0^2 m/2A_1) \times [\omega_2/(\omega_1 + \omega_2)]\, (B/\omega_1)\, J(q)$ for the relativistic cross section.

[8] E. Clementi, IBM J. Res. Dev. **9**, 2 (1965).